Case Report Rapport de cas

Magnetic resonance imaging and immunohistochemistry of primary vertebral hemangiosarcoma in a dog and implications for diagnosis and therapy

Claudia Pérez-Martínez, Marta Regueiro-Purriños, Beatriz Fernández-Martínez, José R. Altónaga, José M. Gonzalo-Orden, María J. García-Iglesias

Abstract — A vertebral mass in a dog with an acute onset paraparesis was identified by magnetic resonance imaging. A poorly differentiated hemangiosarcoma was diagnosed by histopathology and immunohistochemistry. Endothelial nitric oxide synthase could be a new differential marker for poorly differentiated hemangiosarcoma in dogs. Immunohistochemical detection of p53 phosphorylated at Serine[392], p53, CD117, and CD44 suggest targets for design of therapeutic strategies.

Résumé — Imagerie par résonance magnétique et immunistochimie d'un hémangiosarcome vertébral primaire chez un chien et répercussions pour le diagnostic et le traitement. Une masse vertébrale chez un chien atteint d'une manière soudaine d'une paraparésie a été identifiée à l'aide d'imagerie par résonance magnétique. Un hémangiosarcome mal différencié a été diagnostiqué par histopathologie et immunohistochimie. La synthase à l'oxyde nitrique endothélial pourrait être un nouveau marqueur différentiel pour l'hémangiosarcome mal différencié chez les chiens. La détection immunohistochimique de p53 phosphorylé à la sérine[392], p53, CD117 et CD44 suggère des cibles pour la conception de stratégies thérapeutiques.

(Traduit par Isabelle Vallières)

H emangiosarcoma (HSA) is a highly malignant tumor of endothelial cells that can arise in any site with blood vessels. The most common primary sites for this tumor in dogs are the spleen, skin, and subcutaneous tissue and right atrium; primary bone HSAs are uncommon (1). Clinical signs of HSA involving bone include lameness and pain on manipulation of the affected anatomic region; however, they are not pathognomonic for neoplastic disease. Magnetic resonance imaging (MRI) accurately identifies the location and extent of a mass, but the MRI changes for a neoplasm may be similar to MRI findings due to non-neoplastic soft tissue masses (2). Thus, the final diagnosis is based on histological and immunohistological (IHC) studies. However, there is limited information on cellular and molecular features of non-visceral HSA (3).

The aims of this study were to emphasize the importance of considering cancer as a differential diagnosis of lesions detected by MRI in dogs with paraplegia, and to evaluate the expression of IHC markers in a poorly differentiated HSA as suitable tools for its accurate diagnosis and for the identification of molecules which may be used as therapeutic targets of non-visceral HSA in future investigations.

Case description

A 4-year-old male American Staffordshire terrier was evaluated for an acute onset, progressive pelvic limb weakness of 8 days duration. Neurological examination showed marked ambulatory paraparesis, proprioceptive deficits in both hind limbs and normal segmental spinal reflexes. The cutaneous trunci reflex was absent caudal to the first lumbar vertebra. Superficial pain perception was diminished. Based upon neurologic examination, a T3-L3 myelopathy was suspected. Differential diagnoses included disk herniation, vascular lesions, fibrocartilaginous embolism, neoplasms, and inflammatory/infectious diseases. No significant abnormalities were identified in the complete blood (cell) count (CBC), serum biochemistry, urinalysis, two-view thoracic radiograph, and electrocardiogram. Magnetic resonance imaging (MRI) was performed with a high field 3.0T magnet (Signa HDx; GE Healthcare, Madrid, Spain). Technical sequences included: T1-weighted pulse sequences in sagittal and axial planes; T2-weighted pulse sequences [Fast Relaxation Fast Spin Echo sequence (FRFSE); and Gradient Echo sequence (GRE)] and T1 [Spin Echo sequence (SE) post-contrast]. Images in sagittal and axial planes were obtained after intravenous administration of paramagnetic contrast medium

Institute of Biomedicine (IBIOMED) (Pérez-Martínez, García-Iglesias), Department of Veterinary Medicine, Surgery and Anatomy, Veterinary School (Regueiro-Purriños, Altónaga, Gonzalo-Orden), University of León, Spain; Micros Veterinaria, León, Spain (Fernández-Martínez).

Address all correspondence to Dr. Claudia Pérez-Martínez; e-mail: cperm@unileon.es
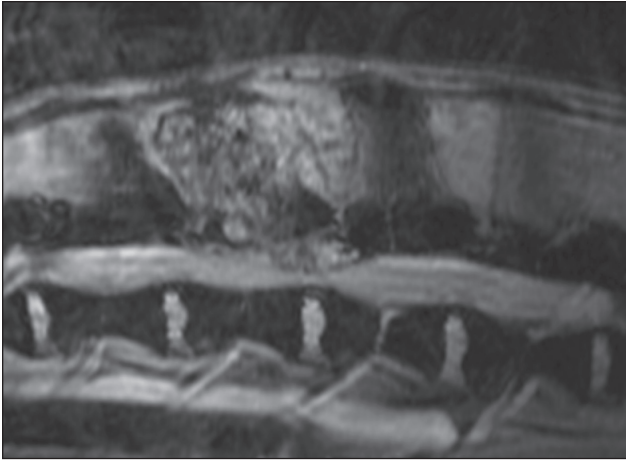
Figure 1. Magnetic resonance image of a hemangiosarcoma in the spine of a dog. A hyperintense mass was identified in the vertebral arch and spinous process of L2 with invasion of the vertebral canal at the L2-L3 disc space. T2 GRE image.

(Optimark; Mallinckrodt Pharmaceuticals, Raleigh, North Carolina, USA), 0.05 mmol/kg body weight (BW), gadoversetamide 0.5 mmol/mL.

A mass was identified in the vertebral arch and spinous process of L2. It invaded the vertebral canal and the L2-L3 disc space, causing dorsolateral compression of the spinal cord. The lesion (4 cm × 2 cm × 4 cm) was hyperintense compared to normal spinal cord and epidural fat on T2-weighted images in FRFSE and T2 GRE images (Figure 1). It was mildly hyperintense on T1-weighted images, and enhanced strongly and homogenously after the administration of contrast. The MRI findings did not allow a definitive diagnosis to be made because, although they were mainly consistent with neoplasia, other etiologies such as epidural hematoma and inflammatory/infectious tumor-like lesions, or osteomyelitis should also be considered.

The animal was euthanized due to its poor quality of life. On necropsy, a 2 cm × 3 cm, ill-defined, hemorrhagic mass was initially identified within the iliopsoas muscle on the right side of the spine. Gross examination of the spine showed an abnormally large L2 vertebra with destruction of normal bone due to the presence of a soft tissue mass which also intruded into the spinal canal, strictly epidural, causing spinal cord compression. The lungs contained disseminated, dark red nodules, 1 to 2 mm in diameter. No gross abnormalities were identified in skin overlying the mass or other organs.

Samples were fixed in 10% neutral buffered formalin, embedded in paraffin, sectioned (4 μm) and stained with hematoxylin and eosin (H&E) and Masson's trichrome stains. Selected sections were immunohistochemically labelled by the avidin-biotin-peroxidase complex (ABC-P) method and double immunofluorescence. Details of the primary antibodies used in this study, including dilutions, are summarized in Table 1.

Microscopically, the highly cellular lesion was composed of cords and solid sheets of pleomorphic cells, which infiltrated myofibers and vertebral bone, resulting in degeneration and necrosis. Neoplastic cells showed ill-defined limits with a single nucleus that ranged from spindle-shaped to reniform

and chromatin from finely stippled to coarse smudged. Nuclear size often differed two-fold or more among tumor cells with presence of 1 prominent nucleolus in the larger ones. The mitotic index was high (4 mitoses per high-power field) and atypical mitotic figures were seen frequently. A few areas of the tumor showed small splits, which were lined by a single layer of plump undifferentiated pleomorphic cells resembling irregular vascular spaces. Masson's trichrome stain revealed the presence of little intercellular collagen in any location in the tumor mass. Multifocal to coalescing foci of hemorrhage and necrosis corresponded to the grossly hemorrhagic appearance of the neoplasm. The pulmonary nodules and 1 small focus (< 1 mm) in the spleen showed similar characteristics to those of the main mass. No lesions were observed in the nerves within the iliopsoas muscle.

Pleomorphic tumor cells were negative for keratin, but positive for vimentin (Table 1) which supported a diagnosis of sarcoma. Almost all the pleomorphic cells exhibited strong expression of CD31 and focal weak labelling for vWf, suggesting a diagnosis of HSA (4). There was no detectable expression of antigens characteristic of glial cells (GFAP), striated muscle (α-sarcomeric actin, desmin), smooth muscle (α-smooth muscle actin, desmin), histiocytes (lysozyme), and T-lymphocytes (CD3); this was important in ruling out the diagnoses of glioma and other sarcomas (Table 1). However, numerous vimentin- and SMA-positive spindle-shaped to oval cells, which were difficult to differentiate morphologically in H&E sections, were arranged in clusters or around the groups of CD31-positive cells (Figure 2). Lack of desmin expression (Table 1) may be useful in differentiating SMA-positive myofibroblasts from pericytes, weakly positive for desmin, and from smooth muscle cells, strongly positive for desmin (5). Endothelial nitric oxide synthase, p53, p53 phosphorylated at Serine[392] and CD117 were expressed in pleomorphic tumor cells and CD44 was expressed in myofibroblasts (Table 1).

Based on overall differentiation and nuclear variation (6) as well as cellular immunostaining, the tumor was categorized as a poorly differentiated hemangiosarcoma with an important supportive component of myofibroblasts. Taking into account the fact that lung and spleen lesions were smaller and composed of CD31-positive pleomorphic cells with few myofibroblasts, the location in the spine was considered the neoproliferative site of origin with muscle invasion and intrusion into the vertebral canal. Foci in lungs and spleen were considered to be early lesions from the spreading of the tumor.

Discussion

This case report is focused on the description of IHC features of primary vertebral HSA, which is relatively uncommon in dogs (1), but must be included in the differential diagnosis for compressive myelopathies (2) because the prognosis and treatment of this clinical manifestation depend on its correct diagnosis. Thus, it is important to obtain information that allows the early detection of this aggressive neoplasm and the identification of potential therapeutic targets (3). The present results support that the IHC detection of CD31 antigen has a greater value than the vWf antigen in the diagnosis of poorly differentiated HSAs, as

Table 1. Immunohistochemical characterization of a vertebral poorly differentiated hemangiosarcoma in a dog

Markers	Source	Titers	Cell expression	
			Pleomorphic cells[a]	Stromal cells[a]
CK8	BD Biosciences[b]	1:5	−	−
CK19	Thermo Fisher[c]	1:10	−	−
Vimentin	Dako[d]	1:1000	+++	+++
CD31	Dako	1:100	+++	−
vWf	Dako	1:1000	+	−
eNOS	Thermo Fisher	1:200	+++	−
SMA	Sigma Aldrich[e]	1:5000	−	+++
Desmin	Thermo Fisher	1:10	−	−
α-sarcomeric actin	Sigma Aldrich	1:2000	−	−
GFAP	Dako	1:5000	−	−
CD3	Dako	1:200	−	−
Lysozyme	Dako	1:100	−	−
CD117	Dako	1:800	+++	−
p53	Biolegend[f]	1:200	+++	−
pp53 Ser[392]	Santa Cruz Biotech[g]	1:100	+++	−
Caspase-3	Cell Signaling[h]	1:300	−	−
CD44	Santa Cruz Biotech	1:400	−	+++

[a] Scoring grades for IHC staining: +++, > 70%; ++, 70% to 31%; +, 30% to 10%; and −, < 10% labelled cells.
[b] BD Biosciences, San Jose, California, USA.
[c] ThermoFisher, Rockford, Illinois, USA.
[d] Dako, Golstrup, Denmark.
[e] Sigma Aldrich, St. Louis, Missouri, USA.
[f] Biolegend, San Diego, California, USA.
[g] Santa Cruz Biotech, Heidelberg, Germany.
[h] Cell Signaling, Danvers, Massachusetts, USA.
CK — cytokeratin; CD — cluster of differentiation; vWf — von Willebrand factor; eNOS — endothelial nitric oxide synthase; SMA — α-smooth muscle actin; GFAP — glial fibrillary acidic protein; pp53 Ser[392] — p53 phosphorylated at Serine[392].
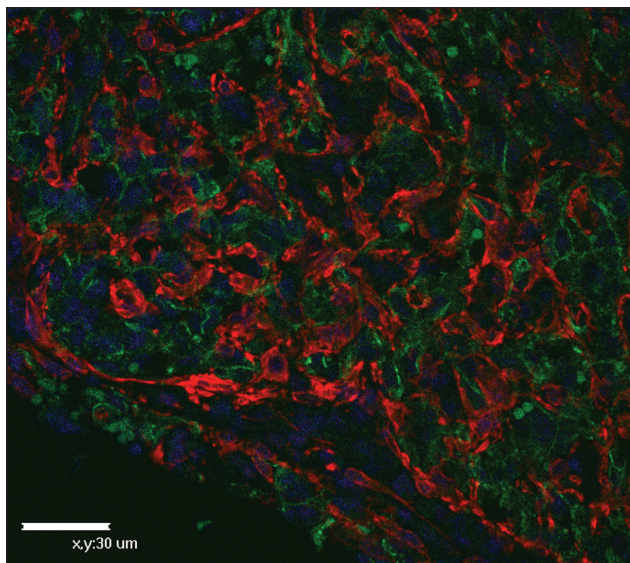
Figure 2. Immunostaining of hemangiosarcoma in the spine of a dog. Clusters of CD31-positive cells are surrounded by numerous SMA-positive myofibroblasts. Double immunofluorescence for CD31 [green, fluorescein isothiocyanate, and SMA (red, rhodamine)] with nuclear DAPI counterstain.

has been previously reported (4). Although CD31 specificity is excellent (4), there are reports of CD31 positivity in human carcinomas and monocytes, which highlights the importance of using a panel of antibodies to aid in avoiding a misdiagnosis (7,8). Furthermore, the lower expression of vWf suggested an origin from endothelial progenitor cells, in which vWf expres-

sion occurs later than CD31 expression (9). The origin of this neoplasm from primitive, poorly differentiated cells is also supported by the immunodetection of c-kit proto-oncogene product (CD117), tyrosine kinase growth factor receptor for stem cell factor, as has been described in an *in vitro* study on canine HSA (10). As such, canine HSA may be expected to respond to tyrosine kinase inhibitors (TKI) and this approach may allow the future development of novel therapies for treatment of HSA in dogs (6,11). However, recent *in vivo* results report that the use of TKI does not improve either disease-free interval or overall survival in dogs with stage I and II splenic HSA (12). These results highlight the need for larger and deeper evaluation of *in vivo* HSA's.

Expression of eNOS in the pleomorphic cells, an enzyme that catalyzes the production of nitric oxide in endothelial cells, suggests that eNOS was a more sensitive marker than vWf in the diagnosis of poorly differentiated HSA, and it also supported an origin from endothelial progenitor cells (13), as did the lack of SMA expression.

The high proliferation index (> 20% tumor cells staining with Ki67) and the negative caspase-3 immunolabelling suggested that the nuclear p53 protein, which is detected in more than 90% of pleomorphic cells, was of a mutant type instead of wild type p53 which induces cell-cycle arrest in G1 or apoptosis. Unlike other reports (14), the present results seem to suggest that inactivation of the p53 pathway might play a role in the pathogenesis of poorly differentiated HSA with invasiveness in dogs, a relationship that has been also described in cows (15). The present study examined the phosphorylation status of Ser[392], which seems to regulate the oncogenic function of

mutant p53 (16). The finding of numerous pleomorphic cells exhibiting p53 phosphorylated at Ser^{392} could indicate that tumors showing this IHC expression pattern may be more sensitive to the cytotoxic effect of radiotherapy and chemotherapy than those expressing the unphosphorylated form of mutant p53 which is more potent in protecting tumor cells (16). Thus, presence of mutant p53 phosphorylated at Ser^{392} could possibly be used to predict the responsiveness to therapy in this type of canine neoplasm, but further research with a larger number of dogs with HSA should be carried out to test this hypothesis.

The use of SMA enabled the identification of numerous myofibroblasts as a previously unrecognized stromal supporting element, an active participant in the progression of the tumor (5). Moreover, the expression of CD44 in the myofibroblasts seems to support critical functions of these stromal cells in the tumor growth which could be blocked as previously described (17); so a potential antitumor substance targeted on this stromal population in poorly differentiated HSAs might provide a basis for therapy.

In summary, the novelty of the current study is the assessment of eNOS for routine diagnosis and of p53 phosphorylated at Ser^{392} for therapy purposes in poorly differentiated HSAs in dogs. Although these results are based on the study of a single case and they should be researched in a large number of dogs, the possibility that eNOS could be used as a new differential marker with greater sensitivity than vWf for the diagnosis of poorly differentiated HSA in dogs should be explored. Furthermore, the positive expression of p53 phosphorylated at Ser^{392}, p53, and CD117 in tumor cells as well as CD44 in myofibroblasts suggests that these proteins might be suitable targets for the development of novel therapeutic approaches to this aggressive disease. Further investigation is required to confirm the significance of these findings. CVJ

References

1. Srebernik N, Appleby EC. Breed prevalence and sites of haemangioma and haemangiosarcoma in dogs. Vet Rec 1991;129:408–409.
2. de la Fuente C, Pumarola M, Añor S. Imaging diagnosis — Spinal epidural hemangiosarcoma in a dog. Vet Radiol Ultrasound 2013;55:424–427.
3. Krump-Konvalinkova V, Kleideiter E, Friedrich U, Klotz U, Kirkpatrick CJ. Tumorigenic conversion of endothelial cells. Exp Mol Pathol 2003;75:154–159.
4. Ferrer L, Fondevila D, Rabanal RM, Vilafranca M. Immunohistochemical detection of CD31 antigen in normal and neoplastic canine endothelial cells. J Comp Pathol 1995;112:319–326.
5. Eyden B. The myofibroblast: Phenotypic characterization as a prerequisite to understanding its functions in translational medicine. J Cell Mol Med 2008;12:22–37.
6. Sabbattini S, Bettini G. An immunohistochemical analysis of canine haemangioma and haemangiosarcoma. J Comp Pathol 2009;140:158–168.
7. Young BR, Frierson HF, Jr, Ly MN, Smith D, Swanson PE. CD31 immunoreactivity in carcinomas and mesotheliomas. Am J Clin Pathol 1998;110:374–377.
8. McKenney JK, Weiss SW, Folpe AL. CD31 expression in intratumoral macrophages: A potential diagnostic pitfall. Am J Surg Pathol 2001;25:1167–1173.
9. Kakiuchi-Kiyota S, Crabbs TA, Arnold LL, et al. Evaluation of expression profiles of hematopoietic stem cell, endothelial cell, and myeloid cell antigens in spontaneous and chemically induced hemangiosarcomas and hemangiomas in mice. Toxicol Pathol 2013;41:709–721.
10. Gorden BH, Kim JH, Sarver AL, et al. Identification of three molecular and functional subtypes in canine hemangiosarcoma through gene expression profiling and progenitor cell characterization. Am J Pathol 2014;184:985–995.
11. Lyles SE, Milner RJ, Kow K, Salute ME. In vitro effects of the tyrosine kinase inhibitor, masitinib mesylate, on canine hemangiosarcoma cell lines. Vet Comp Oncol 2012;10:223–235.
12. Gardner HL, London CA, Portela RA, et al. Maintenance therapy with toceranib following doxorubicin-based chemotherapy for canine splenic hemangiosarcoma. BMC Vet Res 2015;11:131–139.
13. Qiao W, Niu L, Liu Z, Qiao T, Liu C. Endothelial nitric oxide synthase as a marker for human endothelial progenitor cells. Tohoku J Exp Med 2010;221:19–27.
14. Yonemaru K, Sakai H, Murakami M, et al. The significance of p53 and retinoblastoma pathways in canine hemangiosarcoma. J Vet Med Sci 2007;69:271–278.
15. Carvalho T, Naydan D, Nunes T, Pinto C, Peleteiro MC. Immunohistochemical evaluation of vascular urinary bladder tumors from cows with enzootic hematuria. Vet Pathol 2009;46:211–221.
16. Yap DBS, Hsieh JK, Zhong S, et al. Ser392 phosphorylation regulates the oncogenic function of mutant p53. Cancer Res 2004;64:4749–4754.
17. Spaeth EL, Labaff AM, Toole BP, Klopp A, Andreeff M, Marini FC. Mesenchymal CD44 expression contributes to the acquisition of an activated fibroblast phenotype via TWIST activation in the tumor microenvironment. Cancer Res 2013;73:5347–5359.